Journal of Low Temperature Physics, Vol. 147, Nos. 3/4, May 2007 (© 2007)
DOI: 10.1007/s10909-007-9329-6

Symmetries of Pairing Correlations in Superconductor–Ferromagnet Nanostructures

M. Eschrig,[1] T. Löfwander,[1] T. Champel,[1,3] J. C. Cuevas,[1,2,4] J. Kopu,[1] and Gerd Schön[1,2]

[1] *Institut für Theoretische Festkörperphysik and DFG-Center for Functional Nanostructures, Universität Karlsruhe, D-76128 Karlsruhe, Germany*
E-mail: Eschrig@tfp.uni-karisruhe.de
[2] *Forschungszentrum Karlsruhe, Institut für Nanotechnologie D-76021 Karlsruhe, Germany*
[3] *Present address: Laboratoire de Physique et Modélisation des Milieux Condensés, C.N.R.S. 25, avenue des Martyrs, B.P. 166, 38042 Grenoble Cedex, France.*
[4] *Present address: Departamento de Física Teórica de la Materia Condensada C-V, Facultad de Ciencias, Universidad Autónoma de Madrid, 28049 Madrid, Spain.*

Using selection rules imposed by the Pauli principle, we classify pairing correlations according to their symmetry properties with respect to spin, momentum, and energy. We observe that inhomogeneity always leads to mixing of even- and odd-energy pairing components. We investigate the superconducting pairing correlations present near interfaces between superconductors and ferromagnets, with focus on clean systems consisting of singlet superconductors and either weak or half-metallic ferromagnets. Spin-active scattering in the interface region induces all of the possible symmetry components. In particular, the long-range equal-spin pairing correlations have odd-frequency s-wave and even-frequency p-wave components of comparable magnitudes. We also analyze the Josephson current through a half-metal. We find analytic expressions and a universality in the temperature dependence of the critical current in the tunneling limit.

PACS Numbers: *74.45.+c, 74.20.Rp, 74.50.+r.*

1. INTRODUCTION

The rich physics specific for boundary regions between superconducting and ferromagnetic materials has recently been probed in a series of experiments.[1–20] Apart from confirming earlier theoretical predictions[21–24] they provide deep insight into the coexistence of the two types of order and have inspired new ideas in the emerging field of spin electronics. In the boundary region the characteristic correlations known from the proximity

effect in normal metals[25] are induced, but in addition to the usual decay, they show an oscillating behavior. [22] The length scales for decay and oscillations are set by the magnetic length.[23] It is smaller than the decay length in a normal metal, for ballistic systems by the ratio between temperature and exchange energy, k_BT/J, and for diffusive systems by the factor $\sqrt{k_BT/J}$. This leads to modifications of the density of states[26–29] and the Josephson effect through ferromagnets.[30] For usual ferromagnets J is considerably larger than k_BT, and the proximity effect is hard to observe. A breakthrough came with the advance of dilute ferromagnetic alloys with rather low spin polarization, such as $Pd_{1-x}Ni_x$ or $Cu_{1-x}Ni_x$, where magnetic Ni ions are integrated into a non-magnetic matrix. A high level of control has been reached with heterostructures containing such "weak" ferromagnets (low spin polarization). E.g., it became possible to spatially resolve properties on the scale of the magnetic length and to observe the proximity effect.[6,7]

In parallel, it remained an important goal for the further development of spin electronics to create and investigate heterostructures[12–16] where "strong" ferromagnets with large exchange splitting of the bands and high spin polarization are in contact with superconductors. In the extreme case, for so-called half-metallic materials, the polarization reaches values close to 100%. Half metals are metallic in one spin direction with respect to a certain spin quantization axis, and semiconducting or insulating in the other. In the course of this research a so-called "long-range proximity effect" was discovered,[13–15,31–35] which is governed by a length scale typical of the proximity effect in a normal metal, rather than the magnetic length of the ferromagnet involved. Such long-range proximity amplitudes have their origin in the mixing between singlet and triplet pair amplitudes inherent to pairing in the presence of broken spin-rotation symmetry.[32,34,36] Triplet correlations are classified according to their projection on the spin quantization axis that renders the quasiparticle bands in the ferromagnet diagonal. There are three corresponding amplitudes, $m = 0, \pm 1$. Of those the equal spin pair amplitudes, $m = \pm 1$, lead to the long-range proximity effect, as pairing occurs within the same spin band and is unaffected by the large exchange energy J. This explains the penetration of triplet pair amplitudes into the ferromagnet, once they are created.[31–33] However, the questions how they are created in the first place and what are their magnitudes remain active research topics.[31–41]

The creation mechanisms for pairing correlations inside the ferromagnet differ in the ballistic limit significantly for weak and strong ferromagnets. For the following discussion we will concentrate on singlet superconductors. In the case of a weak ferromagnet the singlet superconductor induces in the first place a mixture of singlet and $m = 0$

triplet pairs in the ferromagnet. Both penetrate only on the short magnetic length scale, but various mechanisms may create long-range $m = \pm 1$ triplet components. Examples are (i) a magnetic domain wall near the interface within a distance of the order of the magnetic length;[31,29] or (ii) two ferromagnets with misaligned quantization axes separated by a singlet superconductor with a thickness of the order of the superconducting coherence length;[38,35] or (iii) a spin-active interface that allows for spin-flip processes.[34] In all cases, magnetic inhomogeneities mix the triplet pair components and create the long-range equal-spin pair amplitudes.

In the case of a strong ferromagnet the roles of the ferromagnet and the superconductor are reversed. Here, in the first place the ferromagnet acts as a source for spin-polarization of Cooper pairs in the superconductor. This results in a boundary layer with coexisting singlet and triplet amplitudes near the interface extending about a coherence length into the superconductor. The important mechanisms here are the spin-mixing terms[34,42–46] (often called spin-rotation) in the reflection and transmission amplitudes of the surface scattering matrix. Such spin-mixing effects arise as a consequence of the different matching conditions for spin-up and spin-down wave functions at the interface.[42] Consequently, the creation of triplet pair amplitudes is entirely the result of the interface properties, taking place in an interface region that is of similar size as the magnetic length. Spin-mixing is most effective at interfaces with strong ferromagnets, increasing in strength with growing spin-polarization of the ferromagnet. Long-range triplet components are created when spin-flip centers are present in the interface region. This mechanism even works in the presence of completely polarized ferromagnets, since the triplet correlations are created entirely within the superconductor, and only after their creation penetrate into the ferromagnet.[34] In addition, the magnitude of the triplet correlations at the interface is proportional to that of the singlet amplitude at the interface, and both are insensitive to impurity scattering (in contrast to the decay behavior away from the interface).[47]

For intermediate spin polarizations the two creation mechanisms for triplet pairing, with strengths depending on microscopic details of the interface and domain wall structures in the ferromagnet, compete and are difficult to characterize theoretically. However, the two limiting cases of weak and strong spin polarization can be treated within a controlled approximation, namely the quasiclassical theory of superconductivity.[48,49] It relies on a separation of two energy scales, the superconducting gap Δ and the Fermi energy ϵ_f, and can be extended to superconductor–ferromagnet heterostructures when the exchange energy J lies either in the low- or in the high-energy range, corresponding to weak and strong ferromagnets, respectively. For weak ferromagnets, this means that Fermi

surface properties such as the density of states at the Fermi level in the normal state, N_f, and the Fermi velocity, v_f, remain unchanged to lowest order in the small quasiclassical expansion parameter J/ϵ_f; note that the magnetization of an itinerant ferromagnet (not contacted with a superconductor) is obtained in first order in an expansion in this parameter and is given by $2\mu_B N_f J$, where μ_B is the Bohr magneton. On the other hand, for strong ferromagnets all effective interactions and indeed the quasiparticle band structure itself are strongly modified by the presence of the exchange splitting. It is not possible a priory to describe the crossover between the two limits within quasiclassical theory.

The outline of this article is as follows. In Section 2 we describe how the Pauli principle naturally leads to a classification of superconducting correlations according to their symmetries with respect to spin, momentum, and energy. We then show by presenting two examples that all these types of correlations are indeed induced at superconductor–ferromagnet interfaces. In Section 3.1 we analyze the case of a weak ferromagnet in contact with a singlet superconductor through a spin-active interface barrier. We also illustrate the difference between the spatial dependences of short-range and long-range proximity amplitudes. In Section 3.2 we consider the case of a strong ferromagnet. In particular, we show results for the proximity effect between a singlet superconductor and a half-metal, and for a Josephson junction involving a half metal. We show that an analytic treatment is possible for the case of small transmissions and a small spin-mixing angle. We find that in these limits, a previously discovered[34] low-temperature anomaly in the critical Josephson current is independent of the interface parameters, and is a direct consequence of the different symmetry properties of the pairing correlations compared to the case of a normal metal between two superconductors.

2. SYMMETRY CLASSIFICATIONS

There has been considerable work that formulated the physics of pairing correlations in diffusive ferromagnets in terms of one particular pairing component, that has odd-frequency, s-wave, equal-spin triplet symmetry.[32] The question arises to which extend this component is important for systems with weak or intermediate impurity scattering. We will show in the following chapters that in fact four different symmetry components exist in ballistic heterostructures, and that they are comparable in size. We start with a general classification of pairing correlations.

Superconducting correlations are quantified by the anomalous Green's function

$$\mathcal{F}_{\alpha\beta}(\vec{r}_1, \tau_1; \vec{r}_2, \tau_2) = \left\langle T_\tau \Psi_\alpha(\vec{r}_1, \tau_1) \Psi_\beta(\vec{r}_2, \tau_2) \right\rangle. \tag{1}$$

It is a matrix in spin space and depends on two coordinates and, in the Matsubara technique, on two imaginary times. The Pauli principle requires that this function changes sign when the two particles are interchanged

$$\mathcal{F}_{\alpha\beta}(\vec{r}_1, \tau_1; \vec{r}_2, \tau_2) = -\mathcal{F}_{\beta\alpha}(\vec{r}_2, \tau_2; \vec{r}_1, \tau_1). \tag{2}$$

This well-known condition follows directly from Eq. (1) and the anti-commutation relations for the field operators. For homogeneous systems $\mathcal{F}$ depends only on relative coordinates $\vec{r} = \vec{r}_1 - \vec{r}_2$ and $\tau = \tau_1 - \tau_2$, i.e. it follows $\mathcal{F}_{\alpha\beta}(\vec{r}, \tau) = -\mathcal{F}_{\beta\alpha}(-\vec{r}, -\tau)$, and after Fourier transformations

$$\mathcal{F}_{\alpha\beta}(\vec{p}, \epsilon_n) = -\mathcal{F}_{\beta\alpha}(-\vec{p}, -\epsilon_n). \tag{3}$$

For inhomogeneous systems this equation holds for each set of center coordinates. The symmetry restriction Eq. (3) in spin, momentum $\vec{p}$, and Matsubara frequency, $\epsilon_n = (2n+1)\pi T$, can be satisfied in four different ways, listed in Table I. Analytical continuation to the complex z-plane leads to $\mathcal{F}_{\alpha\beta}(\vec{p}, z) = -\mathcal{F}_{\beta\alpha}(-\vec{p}, -z)$; in particular, retarded and advanced functions are related as $\mathcal{F}^R_{\alpha\beta}(\vec{p}, \epsilon) = -\mathcal{F}^A_{\beta\alpha}(-\vec{p}, -\epsilon)$ (Ref. 50).

The spin part of Eq. (3) can be divided up into singlet and triplet sectors

$$\mathcal{F}_{\alpha\beta}(\vec{p}, \epsilon_n) = \mathcal{F}_s(\vec{p}, \epsilon_n) \left(i\sigma_y\right)_{\alpha\beta} + \vec{\mathcal{F}}_t(\vec{p}, \epsilon_n) \cdot \left(\vec{\sigma}\, i\sigma_y\right)_{\alpha\beta}, \tag{4}$$

where $\vec{\sigma} = (\sigma_x, \sigma_y, \sigma_z)$ is a vector of the three Pauli matrices. The singlet spin matrix $(i\sigma_y)_{\alpha\beta}$ is odd under the interchange $\alpha \leftrightarrow \beta$, while the three triplet matrices $(\vec{\sigma}\, i\sigma_y)_{\alpha\beta}$ are even. Some insight about the symmetries in the momentum- and frequency-domains can be gained by considering the

TABLE I

The Pauli principle, requiring the pair correlation function to be an odd function under the exchange of two electrons, can be met by properties in spin, orbital, or frequency space as follows

Type	Spin	Momentum	Frequency	Overall symmetry
A	Singlet (odd)	Even	Even	Odd
B	Singlet (odd)	Odd	Odd	Odd
C	Triplet (even)	Odd	Even	Odd
D	Triplet (even)	Even	Odd	Odd

equal-time correlator.[51–53] E.g., for the spin-triplet case the Pauli principle imposes that the following sum must vanish

$$\vec{F}_t(\vec{r}=0,\tau=0)=T\sum_{\epsilon_n}\sum_{\vec{p}}\vec{\mathcal{F}}_t(\vec{p},\epsilon_n)=0. \tag{5}$$

When the orbital part is odd the electrons avoid each other in real space, the equal-time correlator $\vec{F}_t(\vec{p},\tau=0)=T\sum_{\epsilon_n}\vec{\mathcal{F}}_t(\vec{p},\epsilon_n)$ can be finite, and the correlator $\vec{\mathcal{F}}_t(\vec{p},\epsilon_n)$ is even in frequency. On the other hand, when the orbital part is even, the correlator $\vec{\mathcal{F}}_t(\vec{p},\epsilon_n)$ is odd in frequency, and electrons avoid each other in time.

We summarize the symmetry classes in Table I. The usual spin singlet s-wave orbital symmetry Bardeen–Cooper–Schrieffer superconductor is of type A, while the spin triplet *p*-wave orbital symmetry superfluid formed in ^{3}He is of type C. Type D was first considered by Berezinskii[51] in connection with early research on superfluid ^{3}He. Finally, type B was considered in connection with unconventional superconductors by Balatsky, Abrahams and others.[52–55]

So far we have only considered the correlation function. In order to obtain the gap function, additional knowledge of the pairing interaction $\lambda(\vec{p},\vec{p}\,',\epsilon_n,\epsilon_n')$ is required (here for the singlet case)

$$\Delta_s(\vec{p},\epsilon_n)=T\sum_{\epsilon_n'}\sum_{p'}\lambda_s(\vec{p},\vec{p}\,',\epsilon_n,\epsilon_n')\mathcal{F}_s(\vec{p}\,',\epsilon_n'). \tag{6}$$

Clearly, the symmetry of the pairing interaction dictates the symmetry of the gap function through the projection of the correlation function in the gap equation. In particular, if the superconducting correlations are odd in frequency a frequency-dependent pairing interaction (due to strong retardation effects) is needed to obtain a non-vanishing gap and a superconducting transition.

TABLE II

The pairing correlations in ballistic superconductor–ferromagnet systems with spin-active interface scattering can be identified with the four types listed in Table I

Eq. (18), singlet:	Even l: even parity, even in frequency	Type A
	Odd l: odd parity, odd in frequency	Type B
Eqs. (19), (20), triplets:	Odd l: odd parity, even-frequency	Type C
	Even l: even parity, odd-frequency	Type D

3. TRIPLET PAIRING IN CLEAN S/F STRUCTURES

3.1. Weak Ferromagnets

To illustrate how triplet correlations are induced we study a superconductor-weak ferromagnet heterostructure in the ballistic transport regime and include spin-active interface scattering. For simplicity we consider temperatures near the superconducting critical temperature; however, the main results of this section require only the pairing amplitudes in the ferromagnet to be small, and apply with minor modifications to any temperature. In this case, within quasiclassical approximation, the anomalous Green's function follows from the (linearized) Eilenberger equations,[48,49]

$$\left(\vec{v}_f \cdot \nabla + 2\epsilon_n\right) f_s = 2\pi\,\Delta\,\mathrm{sgn}(\epsilon_n) - 2iJ\,f_{tz}, \tag{7}$$

$$\left(\vec{v}_f \cdot \nabla + 2\epsilon_n\right) f_{tz} = -2iJ f_s, \tag{8}$$

$$\left(\vec{v}_f \cdot \nabla + 2\epsilon_n\right) \vec{f}_{t\perp} = 0, \tag{9}$$

where v_f denotes the Fermi velocity for the quasiparticles in the respective material. The superconducting gap Δ is non-zero only in the superconductor, while the exchange field J is non-zero only in the ferromagnet. We assume that the ferromagnet has a single domain and use the direction of its exchange field $J\hat{z}$ as spin quantization axis. The spin-active interface can have a different spin-quantization axis, that we denote $\hat{\mu}$ (see below).

The main features of the set of differential equations (7)–(9) are: (i) the inhomogeneity of the equation for f_{tz} requires both J and f_s to be present. Thus, this component naturally emerges in a ferromagnet coupled to a singlet superconductor. (ii) The eigenvalues of the f_s-f_{tz} sub-system for a particular $\vec{v}_f$ are given by $k_n^{\pm} = 2(|\epsilon_n| \pm iJ)/v_f$. Thus, both the singlet f_s and the triplet f_{tz} oscillate on the clean-limit magnetic length scale $\xi_J = v_f/2J$, and decay exponentially on the length scale $\xi_n = v_f/2|\epsilon_n|$; the latter is dominated by the lowest Matsubara frequency, $\epsilon_0 = \pi T$, and occurs on the clean-limit normal-metal coherence length scale $\xi_T = v_f/2\pi T$. (iii) The equation for $\vec{f}_{t\perp} = (f_{tx}, f_{ty})$ is decoupled from the others and is homogeneous. Therefore, the presence of these components requires spin-active interface scattering. (iv) The equations for $\vec{f}_{t\perp}$ do not contain the exchange field, and these components are monotonic decaying functions on the scale ξ_n.

The Eilenberger equations are solved by integrating along trajectories $\vec{v}_f(\vec{p}_f)$ with an initial condition at the starting point of the trajectory. We consider the three-dimensional case and introduce a spherical coordinate system as shown in Fig. 1(b). The superconductor occupies the region $x < 0$, and the ferromagnet the region $x > 0$. We assume rotational invariance around $\hat{x}$, i.e. all quantities will be independent of the variable ϕ_p.

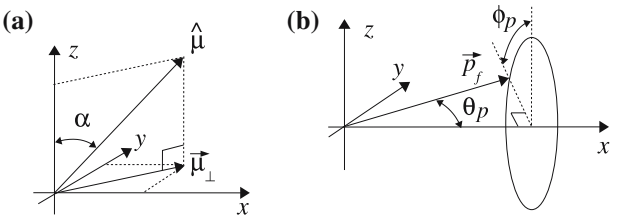

Fig. 1. (a) The spin quantization axis $\hat{\mu}$ of the interface spin-active scattering matrix forms an angle α with the exchange field in the ferromagnet and has a perpendicular component $\vec{\mu}_\perp$. (b) The direction of the momentum $\vec{p}_f$ is expressed in spherical coordinates through the angles θ_p and ϕ_p.

For positive Matsubara frequencies, the initial condition for the trajectories $\theta_p \in [0, \pi/2]$ deep in the superconductor is $f(x \to -\infty) = (\pi\Delta/|\epsilon_n|)i\sigma_y$. For trajectories $\theta_p \in [\pi/2, \pi]$ we start the integration deep in the ferromagnet with initial condition $f(x \to +\infty) = 0$. For negative Matsubara frequencies, the stable direction of integration is the opposite. After applying the boundary conditions described below, the integration proceeds away from the interface.

The boundary conditions at the superconductor–ferromagnet interface for the 2×2 spin matrix Green's functions coincide for positive Matsubara frequencies with those for the retarded functions.[45] Near T_c, they read

$$f_{2,\mathrm{out}} = S_{22} f_{2,\mathrm{in}} \underline{S}_{22}^{\dagger} + S_{21} f_{1,\mathrm{in}} \underline{S}_{21}^{\dagger}, \tag{10}$$

where the indices 1 and 2 refer to the superconducting and ferromagnetic sides, respectively, and 'in' and 'out' denote functions with momenta directed towards or away from the interface. The scattering matrix for holes is written in terms of the scattering matrix for electrons as $\underline{S}_{ij}(\vec{p}_\parallel) = S_{ji}(-\vec{p}_\parallel)^T$. For negative Matsubara frequencies the boundary conditions coincide with the ones for advanced functions, which here simply means interchanging $S \leftrightarrow S^\dagger$ and the side indices ($i \leftrightarrow j$).

For definiteness, we consider a simplified spin-active model in which the scattering matrix is independent of the sign of the parallel momentum $\vec{p}_\parallel$. In this case e.g. the scattering matrix for transmission can be written as[45]

$$S_{12} = S_{21} = e^{i\varphi/2}\left[s_{21} + s'_{21}(\hat{\mu}\cdot\vec{\sigma})\right]\exp\left[i(\hat{\mu}\cdot\vec{\sigma})\vartheta/2\right], \tag{11}$$

where we have an average transmission parameter $s_{21} = (|t_+| + |t_-|)/2$, a spin-filtering transmission parameter $s'_{21} = (|t_+| - |t_-|)/2$, plus a spin-mixing angle ϑ. The amplitudes $t_\pm$ denote the transmission amplitudes of

the interface for the two spin-directions in the basis where $\hat{\mu}\cdot\vec{\sigma}$ is diagonal. The phase φ does not play a role in the following.

For small transmission and small spin mixing the energy gap Δ has a step function form, in which case $f_{1,\mathrm{in}}$ retains its bulk form at the interface. Similarly, the incoming function on the F-side retains its bulk form, i.e. it vanishes $f_{2,\mathrm{in}}=0$. The resulting outgoing amplitude at the interface on the ferromagnetic side can be written as $f_{2,\mathrm{out}}=(A_s+\mathrm{sgn}(\epsilon_n)A_t\,\hat{\mu}\cdot\vec{\sigma})i\sigma_y$, where

$$A_s=A_0\cos\vartheta, \qquad A_t=iA_0\sin\vartheta, \tag{12}$$

and the prefactor is $A_0=|t_+||t_-|\pi\Delta/|\epsilon_n|$. These amplitudes are the initial conditions for the singlet and triplet components in the ferromagnet at the interface. The spatial dependence of all amplitudes can be expressed in terms of the effective coordinate $x_\theta=x/|\cos\theta_p|$. We obtain the following explicit expressions in the ferromagnet

$$f_s(\epsilon_n,x_\theta)=c_s\left[A_s\cos\left(\frac{x_\theta}{\xi_J}\right)-iA_t\cos\alpha\,\sin\left(\frac{x_\theta}{\xi_J}\right)\right]e^{-k_nx_\theta}, \tag{13}$$

$$f_{tz}(\epsilon_n,x_\theta)=c_s\,\mathrm{sgn}(\epsilon_n)\left[A_t\cos\alpha\,\cos\left(\frac{x_\theta}{\xi_J}\right)-iA_s\sin\left(\frac{x_\theta}{\xi_J}\right)\right]e^{-k_nx_\theta}, \tag{14}$$

$$\vec{f}_{t\perp}(\epsilon_n,x_\theta)=c_s\,\mathrm{sgn}(\epsilon_n)\,A_te^{-k_nx_\theta}\,\vec{\mu}_\perp, \tag{15}$$

where $k_n=2|\epsilon_n|/v_f$. Here we introduced the components of $\hat{\mu}$ parallel to the z-axis, $\cos\alpha\,\hat{z}$, and perpendicular, $\vec{\mu}_\perp$, see Fig. 1(a). The coefficient $c_s=\left[1+\mathrm{sgn}(\vec{p}_f\cdot\hat{x})\,\mathrm{sgn}(\epsilon_n)\right]/2$ selects the correct sign of the momentum relative to the x-axis.

We conclude at this stage: (i) the singlet component is purely real while the triplet components are purely imaginary. It follows that in the complex plane $f_s(-z^*)=f_s(z)^*$, $\vec{f}_t(-z^*)=-\vec{f}_t(z)^*$ for each $\vec{p}$. E.g., the retarded functions have the symmetries $f_s^R(-\epsilon)=f_s^R(\epsilon)^*$ and $\vec{f}_t^R(-\epsilon)=-\vec{f}_t^R(\epsilon)^*$. (ii) Spin-mixing (finite ϑ) is crucial for triplet components to be induced at the interface. (iii) The components $\vec{f}_{t\perp}$ are induced only when $\hat{\mu}$ is misaligned with respect to the exchange field (here $J\hat{z}$).

To investigate the symmetry properties we expand the correlation functions in partial waves. Since we have rotational invariance around the $\hat{x}$-axis, and the correlation functions only depend on $\cos\theta_p$ through the projection of the Fermi velocity on the x-axis, we can expand in Legendre polynomials $P_l(\cos\theta_p)$ and get

$$f_s(\cos\theta_p, \epsilon_n, x) = \sum_{l=0}^{\infty} f_s(l, \epsilon_n, x) P_l(\cos\theta_p), \tag{16}$$

$$f_s(l, \epsilon_n, x) = \frac{2l+1}{2} \int_{-1}^{1} d(\cos\theta_p) f_s(\cos\theta_p, \epsilon_n, x) P_l(\cos\theta_p), \tag{17}$$

and similarly for the triplet components. To proceed we have to model the dependencies of the tunneling probabilities and the spin-mixing angle on the trajectory angle and then evaluate the various harmonics. The simplest model is a tunnel cone model with constant transmission probabilities and spin-mixing angle within a range of trajectory angles, i.e. $|t_+(\theta_p)| = \sqrt{\mathcal{T}_+}$, $|t_-(\theta_p)| = \sqrt{\mathcal{T}_-}$, and $\vartheta(\theta_p)$ constant simply called ϑ. In the following we assume a very wide tunnel cone ($\to \pi/2$), but it is straightforward to obtain the expressions for a more narrow cone. After integrations over $\cos\theta_p$ we obtain the amplitudes

$$f_s(l) = A_0 [\mathrm{sgn}(\epsilon_n)]^l [\cos\vartheta \,\mathrm{Re} Q_l(z) - \cos\alpha \sin\vartheta \,\mathrm{Im} Q_l(z)], \tag{18}$$

$$f_{tz}(l) = i A_0 [\mathrm{sgn}(\epsilon_n)]^{l+1} [\cos\alpha \sin\vartheta \,\mathrm{Re} Q_l(z) + \cos\vartheta \,\mathrm{Im} Q_l(z)], \tag{19}$$

$$\vec{f}_{t\perp}(l) = i A_0 [\mathrm{sgn}(\epsilon_n)]^{l+1} [\sin\vartheta \; Q_l(k_n x)] \vec{\mu}_\perp, \tag{20}$$

where $z = k_n^+ x = 2(|\epsilon_n| + iJ)x/v_f$. The function $Q_l(z)$ for the first few l is given by $Q_0(z) = z\Gamma(-1, z)/2$ (s-wave), $Q_1(z) = 3z^2\Gamma(-2, z)/2$ (p-wave), and $Q_2(z) = (5/2)\left[3z^3\Gamma(-3, z)/2 - z\Gamma(-1, z)/2\right]$ (d-wave), where $\Gamma(n, z)$ is the upper incomplete gamma-function. Note the different spatial dependences of the singlet and $m = 0$ triplet on the one hand, and the perpendicular triplets on the other hand, as they enter in the argument of Q_l. Also note that $Q_l(k_n x)$ is purely real since $k_n x$ is real. The Pauli principle and the symmetry requirements it imposes is affirmed in Eqs. (18)–(20). We can also conclude that we have all four types of correlations, see Table II, including equal-spin pairing correlations when $\hat{\mu}$ is not parallel to $\vec{J}$.

In the region $\xi_J \ll x \ll \xi_0$ of the ferromagnet the various components show different decaying behaviors depending on whether the pairing correlations involve two spin bands (f_s and f_{tz}) or only one spin band ($\vec{f}_{t\perp}$). The asymptotic form of the gamma function for $|z| \gg 1$ is $\Gamma(n, z) \sim z^{n-1} e^{-z}$, and we can obtain simplified expressions for $x \gg \xi_J$. We focus on the lowest Matsubara frequency, for which

$$Q_l(z)|_{x \gg \xi_J} \approx -i \frac{2l+1}{2} \frac{\xi_J}{x} e^{-x/\xi_0} e^{-ix/\xi_J}, \tag{21}$$

where $\xi_0 = v_f/2\pi T_c$. The singlet and triplet amplitudes with zero spin-projection have the forms

$$f_s(l) = f_0\left[-\cos\vartheta\,\frac{\sin(x/\xi_J)}{x/\xi_J} + \cos\alpha\,\sin\vartheta\,\frac{\cos(x/\xi_J)}{x/\xi_J}\right]e^{-x/\xi_0}, \quad (22)$$

$$f_{tz}(l) = if_0\left[-\cos\vartheta\,\frac{\cos(x/\xi_J)}{x/\xi_J} - \cos\alpha\,\sin\vartheta\,\frac{\sin(x/\xi_J)}{x/\xi_J}\right]e^{-x/\xi_0}, \quad (23)$$

where the prefactor is $f_0 = \sqrt{\mathcal{T}_+\mathcal{T}_-}(\Delta/T)(2l+1)/2$. Note that there is a $\pi/2$ phase shift between the oscillations of the two components f_s and f_{tz}. Also note that the trajectory resolved functions decay exponentially on the large coherence length scale ξ_0, while the various harmonics decay as $(x/\xi_J)^{-1}$, before the exponential decay on the ξ_0 scale sets in at large distances; the difference comes from the average over trajectories when projecting out the various harmonics. On the other hand, for the perpendicular triplets the asymptotic behavior is not reached until $x \gg \xi_0$, and is of the form

$$\vec{f}_{t\perp}(l) \approx if_0 \sin\vartheta\,\frac{\xi_0}{x}e^{-x/\xi_0}\vec{\mu}_\perp. \quad (24)$$

We plot in Fig. 2 the $l=0$ component of the Green's functions in the ferromagnet, as given by Eqs. (18)–(20) for the lowest Matsubara frequency. The higher order partial waves look very similar and have similar amplitudes. As can be seen in the figure and from Eqs. (22) to (23), in the region $\xi_J \ll x \ll \xi_0$ the correlation functions f_s and f_{tz} decay like $1/x$ and are rapidly reduced by a factor ξ_J/ξ_0 compared to $\vec{f}_{t\perp}$. A similar decay for $\vec{f}_{t\perp}$ is absent in that region. For $x \gg \xi_0$ all components continue to decay according to $x^{-1}e^{-x/\xi_0}$, as can be inferred from Eqs. (22) to (24).

In fact, the Pauli principle requires odd-frequency amplitudes to be present in any inhomogeneous superconducting state, not necessarily spin-polarized. For example, the case of a normal metal coupled to a superconductor is easily obtained from the above calculations and we recover for the case of a usual tunnel barrier (no spin-active scattering) the usual proximity effect.[25] There is only a singlet component of the Green's function and in the normal metal region it can be expressed in terms of partial waves as

$$f_s(l) = \mathcal{T}\frac{\pi\Delta}{|\epsilon_n|}[\mathrm{sgn}(\epsilon_n)]^l\,Q_l\left(\frac{2|\epsilon_n|x}{v_f}\right), \quad (25)$$

which for large distances from the interface $x \gg \xi_0$ decays as $\sim(\xi_0/x)$ $\exp(-x/\xi_0)$. Above we introduced $\mathcal{T}$, the transparency of the interface within the tunnel cone (here for simplicity chosen very wide $\to \pi/2$ as above). We see that higher partial waves $l \geq 1$ are induced, as is always

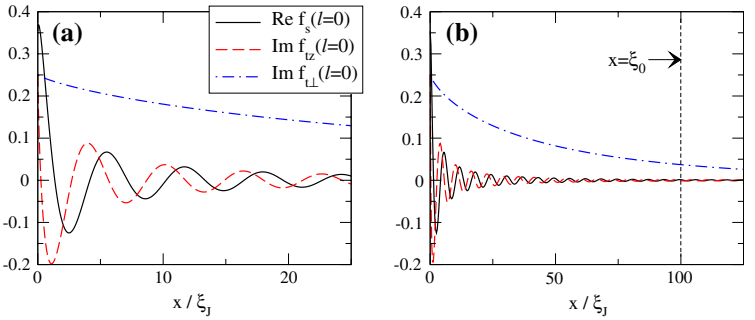

Fig. 2. (Color online) Pair correlation functions in the ferromagnet of a ballistic superconductor–ferromagnet junction. The first partial wave ($l = 0$) for the lowest Matsubara frequency, $\epsilon_0 = \pi T$, is shown. (a) For the singlet, f_s, and triplet with zero spin-projection on the exchange field, f_{tz}, we observe a $1/x$-decay and oscillations, both on the scale $\xi_J = v_f/2J$. On the same scale the perpendicular triplet $f_{t\perp}$ only varies slowly. (b) At large distances all components decay on the coherence length scale ξ_0. However, the magnitudes of f_s and f_{tz} are considerably reduced compared with $f_{t\perp}$ before this region is reached. We have chosen $\xi_0 = 100\xi_J$, $\alpha = \pi/4$, $\vartheta = \pi/4$, and we have normalized the functions by $(\Delta/T)\sqrt{T_+T_-}$.

the case in inhomogeneous systems. In accordance with the Pauli principle, all odd components ($l = 1, 3, \ldots$) are odd in frequency. Thus, both singlet entries (types A and B) in Table I are always present in the usual proximity effect, and in fact in any inhomogeneous singlet superconducting state. Analogously, the two triplet entries (types C and D) in Table I are characteristic for any inhomogeneous triplet superconducting state.

3.2. Half-metallic Ferromagnet

In this section we analyze the various symmetry components, introduced in the previous sections, for the case of a superconductor coupled to a half-metallic ferromagnet. This case was previously studied on theoretical grounds, and a non-zero Josephson-effect was predicted for a superconductor/half-metal/superconductor junction.[34] The effect has recently been confirmed experimentally.[15] In our previous article we focused on the p-wave triplet amplitudes, but it should be noted that there is also an odd-frequency s-wave triplet amplitude present in the half-metal. In fact, within our model all symmetry classes discussed in the previous chapter and shown in Table I are present in the heterostructure. In the following we discuss the results for the clean case. We have performed calculations with impurity scattering ranging from the clean limit to the diffusive limit and have confirmed that both the even-frequency p-wave triplet and the

odd-frequency s-wave triplet components are always present and important for the Josephson current through the half metal.[47]

The full scattering matrix for our model is a 3×3 matrix, where the three scattering channels are the two spin channels in the superconductor and one metallic spin channel in the half metal. The second spin channel in the half metal is insulating and is not participating actively in transport phenomena. As discussed in the introduction, quasiclassical theory is therefore applicable. To be specific, we parameterize the scattering matrix connecting incoming to outgoing waves in the superconductor (S) and half-metallic (F) sides as[34]

$$\hat{\mathbf{S}} = \left(\begin{array}{c|c} r^S & t^{SF} \\ \hline t^{FS} & -r^F \end{array}\right) = \left(\begin{array}{cc|c} r_{\uparrow\uparrow} e^{\frac{i}{2}\vartheta} & r_{\uparrow\downarrow} e^{i(\vartheta_{\uparrow\uparrow}-\vartheta_{\downarrow\uparrow})} & d_{\uparrow\uparrow} e^{i(\vartheta_{\uparrow\uparrow}+\frac{\vartheta}{4})} \\ r_{\downarrow\uparrow} e^{-i(\vartheta_{\uparrow\uparrow}-\vartheta_{\downarrow\uparrow})} & r_{\downarrow\downarrow} e^{-\frac{i}{2}\vartheta} & d_{\downarrow\uparrow} e^{i(\vartheta_{\downarrow\uparrow}-\frac{\vartheta}{4})} \\ \hline d_{\uparrow\uparrow} e^{-i(\vartheta_{\uparrow\uparrow}-\frac{\vartheta}{4})} & d_{\downarrow\uparrow} e^{-i(\vartheta_{\downarrow\uparrow}+\frac{\vartheta}{4})} & -\underline{r}_{\uparrow\uparrow} \end{array}\right), \tag{26}$$

where the extra phases of the transmission amplitudes ensure the unitarity of the scattering matrix, and the magnitudes are given by $r_{\uparrow\uparrow} = 1 - t_{\uparrow\uparrow}^2/2W$, $r_{\downarrow\downarrow} = 1 - t_{\downarrow\uparrow}^2/2W$, $r_{\uparrow\downarrow} = r_{\downarrow\uparrow} = -t_{\uparrow\uparrow} t_{\downarrow\uparrow}/2W$, $\underline{r}_{\uparrow\uparrow} = 1 - (t_{\uparrow\uparrow}^2 + t_{\downarrow\uparrow}^2)/2W$, $d_{\uparrow\uparrow} = t_{\uparrow\uparrow}/W$, and $d_{\downarrow\uparrow} = t_{\downarrow\uparrow}/W$, with $W = 1 + (t_{\uparrow\uparrow}^2 + t_{\downarrow\uparrow}^2)/4$. The five real parameters of the scattering matrix above are $t_{\uparrow\uparrow}$, $t_{\downarrow\uparrow}$, ϑ, $\vartheta_{\uparrow\uparrow}$ and $\vartheta_{\downarrow\uparrow}$.

In the following we derive analytic expressions for a well-defined limiting case: the case of weak transmissions in all channels and small spin mixing angle. In the above scattering matrix this means that ϑ, $t_{\uparrow\uparrow}$ and $t_{\downarrow\uparrow}$ are small. Thus, in this limit the scattering matrix assumes the form

$$\hat{\mathbf{S}}_0 = \left(\begin{array}{cc|c} e^{\frac{i}{2}\vartheta} & 0 & t_{\uparrow\uparrow} e^{i(\vartheta_{\uparrow\uparrow}+\frac{\vartheta}{4})} \\ 0 & e^{-\frac{i}{2}\vartheta} & t_{\downarrow\uparrow} e^{i(\vartheta_{\downarrow\uparrow}-\frac{\vartheta}{4})} \\ \hline t_{\uparrow\uparrow} e^{-i(\vartheta_{\uparrow\uparrow}-\frac{\vartheta}{4})} & t_{\downarrow\uparrow} e^{-i(\vartheta_{\downarrow\uparrow}+\frac{\vartheta}{4})} & -1 \end{array}\right). \tag{27}$$

Before presenting the results, we comment on the parameters in the scattering matrix. Within our theory, the scattering matrix is a phenomenological input that characterizes the scattering of quasiparticles near the Fermi surface on either side of the interface of the system. Microscopic details of the interfaces are irrelevant for the low-energy physics near the Fermi surfaces. Thus, all the parameters are assumed to be independent of

energy, and only depend on the positions of the scattering momenta on the Fermi surface. For strong ferromagnets, J is not a small quantity, and consequently the scattering matrix has spin-active scattering terms of the order of J/ϵ_f, with ϵ_f the Fermi energy. Whereas the spin-mixing angle ϑ is a robust property of any interface to a strong ferromagnet, the spin-flip parameters $t_{\downarrow\uparrow}$, $\vartheta_{\downarrow\uparrow}$ require breaking of spin-rotation symmetry around the quantization axis of the ferromagnet. This can be the result of various mechanisms, for example the presence of interface regions with misaligned spin (magnetic grain layers). The above mentioned parameters represent in this case averages over the grain configuration along the contact region of the interface for each given sample, $t_{\downarrow\uparrow}e^{i\vartheta_{\downarrow\uparrow}} = \langle t_{\downarrow\uparrow}^{(i)} e^{i\vartheta_{\downarrow\uparrow}^{(i)}} \rangle_i$, where i numbers the different grains. Thus, there are expected sample-to-sample variations in the spin-flip parameters unless the typical grain size exceeds the contact size.

We now proceed with the derivation of analytic expressions for the various symmetry components of the pairing amplitudes. On the superconducting side of an interface with a half metal, all four components listed in Table I are induced and can be calculated perturbatively in the small parameters ϑ, $t_{\uparrow\uparrow}$ and $t_{\downarrow\uparrow}$. In the following we denote $\Omega_n = \sqrt{\epsilon_n^2 + |\Delta|^2}$. We obtain for type D: $f_{tz}^D = i\pi\vartheta\epsilon_n\Delta/2\Omega_n^2$, for type C: $f_{tz}^C = -i\pi\vartheta\Delta/2\Omega_n$. In an expansion in spherical harmonics the two components f_{tz}^D and f_{tz}^C correspond to s-wave and p-wave triplets. The type B component only enters in second order in ϑ, and has the form $f_s^B = \pi\vartheta^2\epsilon_n\Delta/4\Omega_n^2$. Finally, the renormalization of the type A singlet component, $\delta f_s^A = -\pi\vartheta^2\epsilon_n^2\Delta/4\Omega_n^3$, reduces the leading component only in second order in ϑ. Consequently, to linear order in ϑ the self-consistent singlet order parameter Δ is not affected and stays constant up to the interface. All components, δf_s^A, f_s^B, f_{tz}^C, and f_{tz}^D decay into the superconductor exponentially with a decay length given by $\xi_n^{(S)} = v_f/2\Omega_n$.

Next we consider the equal spin pairing amplitudes in a symmetric Josephson junction with a half metal of length L extending from $-L/2 < x < L/2$. On either side of the half metal are singlet superconductors with order parameters $|\Delta|e^{i\chi_1}$ and $|\Delta|e^{i\chi_2}$. The equal spin pairing amplitudes in the half metal, $f_{\uparrow\uparrow}$ are proportional to the components f_{tz} in the superconductors. For the even-frequency triplet amplitude we obtain in the half metal

$$f_{\uparrow\uparrow}^C = -i\,\beta_n\,\mathrm{sgn}(\cos\theta_p)\left(\frac{\sinh\frac{k_n x}{\mu}}{\sinh\frac{k_n L}{2\mu}}(e^{i\tilde{\chi}_2}+e^{i\tilde{\chi}_1}) + \frac{\cosh\frac{k_n x}{\mu}}{\cosh\frac{k_n L}{2\mu}}(e^{i\tilde{\chi}_2}-e^{i\tilde{\chi}_1})\right), \tag{28}$$

and for the odd-frequency triplet amplitude

$$f^D_{\uparrow\uparrow} = i\,\beta_n\,\mathrm{sgn}(\epsilon_n)\left(\frac{\cosh\frac{k_n x}{\mu}}{\sinh\frac{k_n L}{2\mu}}(e^{i\tilde{\chi}_2}+e^{i\tilde{\chi}_1})+\frac{\sinh\frac{k_n x}{\mu}}{\cosh\frac{k_n L}{2\mu}}(e^{i\tilde{\chi}_2}-e^{i\tilde{\chi}_1})\right), \quad (29)$$

where $k_n = 2|\epsilon_n|/v_f$, $\mu = |\cos\theta_p|$, and $\beta_n = \pi t_{\uparrow\uparrow} t_{\downarrow\uparrow}\vartheta|\Delta||\epsilon_n|/2(\epsilon_n^2+|\Delta|^2)$. The superconducting phases are renormalized by the phase shifts during tunneling, and are given by $\tilde{\chi}_i = \chi_i - \vartheta_{i,\uparrow\uparrow} - \vartheta_{i,\downarrow\uparrow}$ with $i = 1, 2$. Note that equal-spin amplitudes are only possible when both $t_{\downarrow\uparrow} \neq 0$ and $\vartheta \neq 0$. Even and odd frequency (i.e. p-wave and s-wave) triplets at the interfaces ($x = \pm L/2$) are comparable in size.

To illustrate the different symmetry components, we show in Fig. 3 numerical results for a superconductor/half-metal/superconductor junction. For these results we do not expand the interface scattering matrix in ϑ, $t_{\uparrow\uparrow}$, $t_{\downarrow\uparrow}$ as in Eq. (27), but use the general scattering matrix (26) and solve the boundary conditions numerically.[34] We allow for an angular variation with respect to the interface normal of both the spin mixing angle and the transmission amplitudes; for definiteness we assume a variation proportional to $|\cos\theta_p|$. We iterate the order parameter and the boundary conditions until self-consistency is achieved. We discuss first results for a π-junction ($\tilde{\chi}_1 = 0$, $\tilde{\chi}_2 = \pi$) as this is the ground state of the Josephson junction.[34] To quantify the spatial dependences of the different symmetry amplitudes, we define the functions

$$F_{\alpha\beta}(x) = \frac{2}{\pi}T\sum_{\epsilon_n>0}\left\langle P_l(\cos\theta_p)\, f_{\alpha\beta}(\epsilon_n, x, \theta_p)\right\rangle_{\vec{p}} f_h^*(\epsilon_n), \quad (30)$$

where $P_l(\cos\theta_p)$ is chosen to project out the s-wave (l=0) or p-wave (l = 1) parts of the pairing amplitudes, and $f_h(\epsilon_n) = \pi\Delta/\Omega_n$ is the propagator for a homogeneous singlet superconductor that is introduced here to ensure convergence at large ϵ_n (note that at the boundary points $f_{\alpha\beta}(\epsilon_n)$ decays weakly $\sim 1/\epsilon_n$). As is shown in Fig. 3, on the superconducting side all possible symmetry components listed in Table I are induced, of which the even-frequency p-wave triplet and the odd-frequency s-wave triplet penetrate into the half metal. The latter two components are of similar magnitude, however the p-wave triplet is larger in the center region of the junction than the s-wave triplet. We have also performed calculations including impurity scattering and have shown that *both* components are essential for the Josephson current in the entire range from the ballistic to the diffusive limit. Details will be presented in a forthcoming publication.[47] Also seen in Fig. 3 is that there are different symmetries with respect to the spatial coordinate, that result from the symmetry of the Josephson junction. The components shown are for the ground state; with

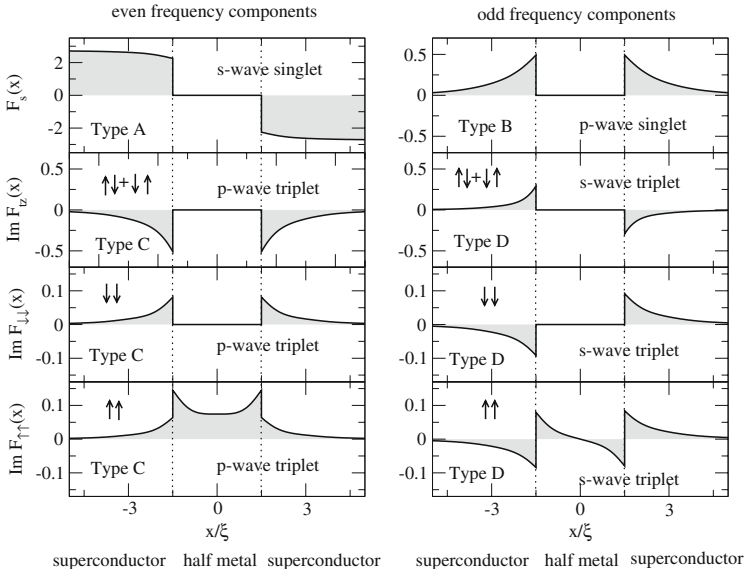

Fig. 3. Spatial dependences of all components of the pairing amplitude for a symmetric superconductor/half-metal/superconductor Josephson π-junction with interfaces characterized by the scattering matrix Eq. (27). The interfaces are indicated by the dashed lines. The components were numerically iterated until self-consistency with the singlet order parameter was achieved. The interface parameters for normal impact angle are $\vartheta = 0.3\pi$, $t_{\uparrow\uparrow} = 1$, $t_{\downarrow\uparrow} = 0.7$, $\vartheta_{\uparrow\uparrow} = \vartheta_{\downarrow\uparrow} = 0$, and the temperature is $T = 0.2T_c$.

a finite Josephson current ($\tilde{\chi}_2 - \tilde{\chi}_1 \neq 0, \pi$) all amplitudes become complex and the spatial symmetries are lost, as can also be inferred from Eqs. (28) to (29). Note that in Fig. 3, as consequence of higher order terms in the transmission parameters and the spin-mixing angle, there are equal-spin pairing correlations also in the superconducting regions, and there are noticeable inhomogeneous contributions to the singlet amplitudes as well.

For comparison, we present in Fig. 4 the pairing components for the zero-junction case ($\tilde{\chi}_1 = \tilde{\chi}_2 = 0$). In this case, the spatial symmetries are opposite to that of the π-junction. We have verified that the π junction has lower free energy.[34]

We consider next the Josephson current through the junction. We assume identical interface parameters for both contacts, that may depend on the impact angle θ_p via a parameter $\mu = |\cos\theta_p|$. We obtain for small ϑ, $t_{\uparrow\uparrow}$, and $t_{\downarrow\uparrow}$ the following expression for the Josephson current density

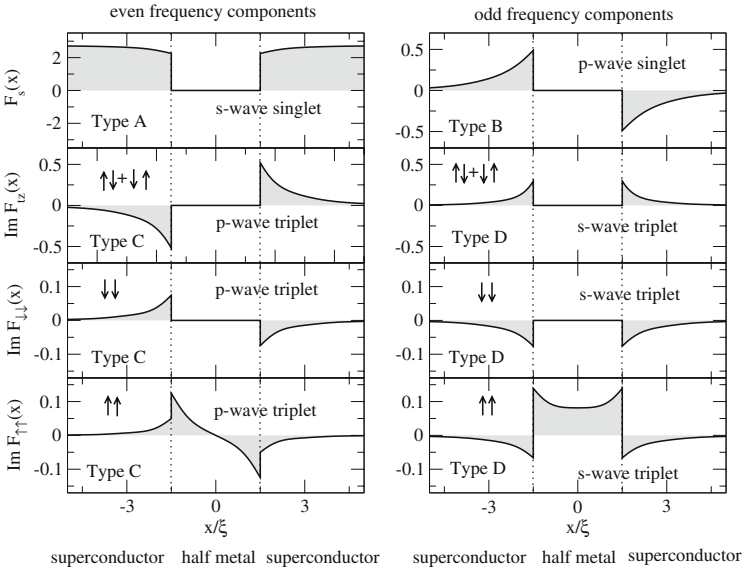

Fig. 4. The same as in Fig. 3, but for zero phase difference.

$$J = -J_c \sin(\tilde{\chi}_2 - \tilde{\chi}_1) \tag{31}$$

$$J_c = eN_f v_f |\Delta|^2 \pi T \sum_{\epsilon_n > 0} \left\langle \frac{\mu\, \vartheta^2 |t_{\downarrow\uparrow}|^2 |t_{\uparrow\uparrow}|^2}{2 \sinh\left(\frac{2\epsilon_n L}{v_f \mu}\right)} \right\rangle_\mu \frac{\epsilon_n^2}{(\epsilon_n^2 + |\Delta|^2)^2}, \tag{32}$$

where $\langle \cdots \rangle_\mu = \int_0^1 d\mu(\ldots)$, and N_f denotes the density of states of the spin-up electrons at the Fermi level in the half metal. We point out several differences to the case of the Josephson effect through a normal metal: (i) the minus sign suggests that the π-junction is stable for all temperatures and parameters within the above approximation. (ii) The Josephson current is proportional to the square of the spin-mixing angle ϑ and the squares of both the tunneling amplitudes $t_{\downarrow\uparrow}$ and $t_{\uparrow\uparrow}$. Thus, the *magnitude* of the critical current is much more sensitive to the interface characteristics than in a usual Josephson junction; in particular, strong sample-to-sample fluctuations are expected as the magnitude is proportional to $t_{\downarrow\uparrow}$. (iii) The additional phases $\vartheta_{\downarrow\uparrow} + \vartheta_{\uparrow\uparrow}$ in $\tilde{\chi}_{1,2}$ can lead to a shift of the equilibrium phase difference between the superconductors except when they are identical for both interfaces of the Josephson junction. (iv) The Josephson current density is a result of both the even-frequency p-wave triplet and the odd-frequency s-wave triplet amplitudes, and neither of them can be neglected.

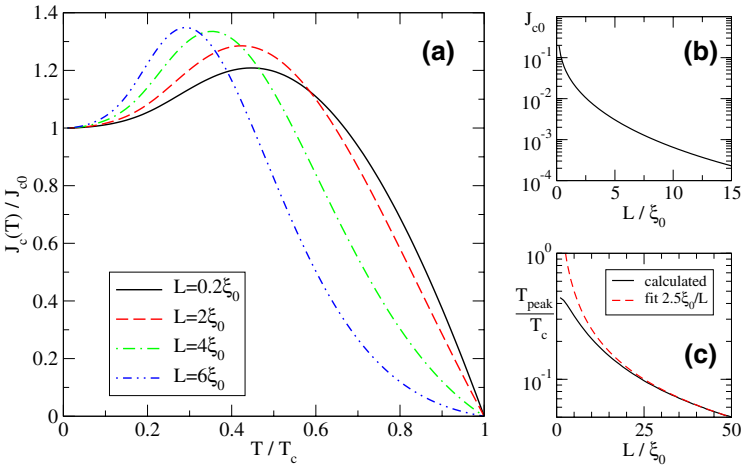

Fig. 5. (Color online) (a) The normalized critical Josephson current density $J_c(T)/J_{c0}$ as computed from Eq. (32) as a function of temperature T. The temperature dependence of the gap is given by the well-known BCS formula. (b) The zero temperature value $J_{c0} = J_c(T=0)$ is shown in units of $eN_f v_f T_c |t_{\downarrow\uparrow}|^2 |t_{\uparrow\uparrow}|^2 \vartheta^2$ as function of junction length L. (c) The peak position of the curves in (a) as function of L.

In Fig. 5(a) we show $J_c(T)$ from Eq. (32) normalized to its zero temperature value. As above we assumed a variation of ϑ, $|t_{\uparrow\uparrow}|$, and $|t_{\downarrow\uparrow}|$ with impact angle that is proportional to $|\cos\theta_p|$. As can be seen, there is a low-temperature anomaly in $J_c(T)$ that has been discussed previously.[34] Here we show that this anomaly is a robust feature that exists even in the limit of small transmission and small spin-mixing angle, and is independent of these material parameters. Thus, the dependence on the interface parameters can be divided out and $J_c(T)/J_c(0)$ is a universal function, only dependent on L/ξ_0. The appearance of the anomaly can be traced back to the different energy dependence of the pair amplitudes in the half metal compared with a normal metal, which results in the ϵ_n^2-factor in the numerator of Eq. (32). The position of the peak maximum in the temperature dependence of the Josephson current is shown in Fig. 5(c) as a function of junction length L. It scales at large L as $T_{\rm peak}/T_c \approx 2.5\xi_0/L$. For small L it saturates at a finite temperature. We also show in Fig. 5(b) the variation of the zero temperature Josephson current with junction length. It decays for lareg L, as is $L^{-1}exp(-L/\xi_0)$.

4. SUMMARY

In conclusion, we have investigated the superconducting pairing correlations with unconventional symmetries at interfaces between superconductors and ferromagnets. We have demonstrated that in ballistic superconductor/ferromagnet junctions spin-active interface scattering naturally leads to all possible symmetry components of pairing amplitudes compatible with the Pauli principle. We have also discussed the case of a junction with a half-metallic ferromagnet. In this case odd-frequency s-wave and even frequency p-wave components are of comparable magnitude and are essential for the Josephson current. This leads to a π-junction, where the supercurrent is carried by spin-triplet Cooper pairs. We have shown that a low-temperature anomaly in the Josephson effect through a half-metal is of universal nature in the tunneling limit in ballistic systems. We have derived analytic expressions for all pairing components and for the Josephson current in the limit of small interface transmissions and small spin-mixing angle.

ACKNOWLEDGEMENTS

We acknowledge stimulating discussions with H. von Löhneysen, D. Beckmann, V. Chandrasekhar, G. Goll, F. Pérez-Willard, C. Sürgers, and H.B. Weber, on the properties of superconductor–ferromagnet heterostructures, and with T. Klapwijk on the observation of triplet supercurrents in a half-metal. Our work was also supported by the German-Israeli Foundation for Scientific Research and Development (J.K.), and the Alexander von Humboldt Foundation (T.L.).

REFERENCES

1. H. von Löhneysen *et al.*, *Annalen d. Physik* **14**, 591 (2005).
2. D. Beckmann, H. B. Weber, and H. von Löhneysen, *Phys. Rev. Lett.* **93**, 197003 (2004); D. Beckmann and H. von Löhneysen, *cond-mat*/0609766 (2006).
3. F. Pérez-Willard, J. C. Cuevas, C. Sürgers, P. Pfundstein, J. Kopu, M. Eschrig, and H. von Löhneysen, *Phys. Rev. B* **69**, 140502 (2004).
4. M. Schöck, C. Sürgers, and H. von Löhneysen, *Eur. Phys. J. B* **14**, 1 (2000).
5. C. Strunk, C. Sürgers, U. Paschen, and H. von Löhneysen, *Phys. Rev. B* **49**, 4053 (1994).
6. T. Kontos *et al.*, *Phys. Rev. Lett.* **86**, 304 (2001); T. Kontos *et al.*, *Phys. Rev. Lett.* **89**, 137007 (2002).
7. V. V. Ryazanov *et al.*, *Phys. Rev. Lett.* **86**, 2427 (2001); V. V. Ryazanov *et al.*, *Phys. Rev. B* **65**, 020501(R) (2001).
8. Y. Blum, M. K. A. Tsukernik, and A. Palevski, *Phys. Rev. Lett.* **89**, 187004 (2002); V. Shelukhin *et al.*, *Phys. Rev. B* **73**, 174506 (2006).
9. H. Sellier *et al.*, *Phys. Rev. Lett.* **92**, 257005 (2004).
10. A. Bauer *et al.*, *Phys. Rev. Lett.* **92**, 217001 (2004).
11. W. Guichard *et al.*, *Phys. Rev. Lett.* **90**, 167001 (2003).

12. M. D. Lawrence and N. Giordano, *J. Phys.: Condens. Matter* **8**, 563 (1996); *ibid* **11**, 1089 (1996).
13. M. Giroud *et al.*, *Phys. Rev. B* **58**, R11872 (1998); M. Giroud *et al.*, *Eur. Phys. J. B* **31**, 103 (2003).
14. V. T. Petrashov *et al.*, *Phys. Rev. Lett.* **83**, 3281 (1999).
15. R. S. Keizer *et al.*, *Nature* **439**, 825 (2006).
16. J. Aumentado and V. Chandrasekhar, *Phys. Rev. B* **64**, 054505 (2001).
17. J. Y. Gu *et al.*, *Phys. Rev. Lett.* **89**, 267001 (2002).
18. J. M. E. Geers *et al.*, *Phys. Rev. B* **64**, 094506 (2001).
19. S. M. Frolov *et al.*, *Phys. Rev. B* **70**, 144505 (2004).
20. D. Stamopoulos and M. Pissas, *Phys. Rev. B* **73**, 132502 (2006).
21. L. N. Bulaevskii, V. V. Kuzii, and A. A. Sobyanin, *Pis'ma Zh. Eksp. Teor. Fiz.* **25**, 314 (1977) [*JETP Lett.* **25**, 290 (1077)].
22. A. I. Buzdin, L. N. Bulaevskii, and S. V. Panyukov, *Pis'ma Zh. Eksp. Teor. Fiz.* **35**, 147 (1982) [*JETP Lett.* **35**, 178 (1982)].
23. L. N. Bulaevskii *et al.*, *Adv. Phys.* **34**, 175 (1985).
24. Z. Radovic *et al.*, *Phys. Rev. B* **44**, 759 (1991).
25. P. G. de Gennes, *Rev. Mod. Phys.* **36**, 225 (1964); V. G. Kogan, *Phys. Rev. B* **26**, 88 (1982).
26. M. Zareyan, W. Belzig, and Yu. V. Nazarov, *Phys. Rev. Lett.* **86**, 308 (2001).
27. K. Halterman and O. T. Valls, *Phys. Rev. B* **65**, 14509 (2002).
28. T. Yokoyama, Y. Tanaka, and A. A. Golubov, *Phys. Rev. B* **73**, 094501 (2006).
29. A. Konstandin, J. Kopu, and M. Eschrig, *Phys. Rev. B* **72**, 140501(R) (2005).
30. A. A. Golubov, M. Yu. Kupriyanov, and E. Il'ichev, *Rev. Mod. Phys.* **76**, 411 (2004).
31. F. S. Bergeret, A. F. Volkov, and K. B. Efetov, *Phys. Rev. Lett.* **86**, 4096 (2001).
32. F. S. Bergeret, A. F. Volkov, and K. B. Efetov, *Rev. Mod. Phys.* **77**, 1321 (2005).
33. A. Kadigrobov, R. I. Shekhter, and M. Jonson, *Europhys. Lett.* **54**, 394 (2001).
34. M. Eschrig *et al.*, *Phys. Rev. Lett.* **90**, 137003 (2003); J. Kopu *et al.*, *Phys. Rev. B* **69**, 094501 (2004). M. Eschrig *et al.*, in *Adv. in Sol. State Phys.* B. Kramer, ed., Springer Verlag Heidelberg (2004), vol. 44, pp. 533–546.
35. T. Löfwander *et al.*, *Phys. Rev. Lett.* **95**, 187003 (2005); T. Löfwander, T. Champel, and M. Eschrig, *cond-mat*/0605172 (2006).
36. T. Champel and M. Eschrig, *Phys. Rev. B* **71**, 220506(R) (2005); *ibid.* **72**, 054523 (2005).
37. T. T. Heikkilä, F. K. Wilhelm, and G. Schön, *Europhys. Lett.* **51**, 434 (2000).
38. Y. V. Fominov, A. A. Golubov, and M. Y. Kupriyanov, *JETP Lett.* **77**, 510 (2003).
39. A. I. Buzdin, *Rev. Mod. Phys.* **77**, 935 (2005).
40. V. Braude and Yu. V. Nazarov, *cond-mat*/0610037.
41. Y. Asano, Y. Tanaka, and A. A. Golubov, *cond-mat*/0609566.
42. T. Tokuyasu, J. A. Sauls, and D. Rainer, *Phys. Rev. B* **38**, 8823 (1988).
43. M. Fogelström, *Phys. Rev. B* **62**, 11812 (2000).
44. Yu. S. Barash and I. V. Bobkova, *Phys. Rev. B* **65**, 144502 (2002).
45. E. Zhao, T. Löfwander, and J. A. Sauls, *Phys. Rev. B* **70**, 134510 (2004).
46. A. Cottet and W. Belzig, *Phys. Rev. B* **72**, 180503(R) (2005).
47. M. Eschrig and T. Löfwander, to be published.
48. G. Eilenberger, *Z. Phys.* **214**, 195 (1968).
49. A. I. Larkin and Y. N. Ovchinnikov, *Sov. Phys. JETP* **28**, 1200 (1969).
50. See for example J. W. Serene and D. Rainer, *Phys. Rep.* **101**, 221 (1983).
51. V. L. Berezinskii, *Pis'ma Zh. Eksp. Teor. Fiz.* **20**, 628 (1974) [*JETP Lett.* **20**, 287 (1974)].
52. A. Balatsky and E. Abrahams, *Phys. Rev. B* **45**, 13125 (1992).
53. E. Abrahams *et al.*, *Phys. Rev. B* **52**, 1271 (1995).
54. P. Coleman, E. Miranda, and A. Tsvelik, *Phys. Rev. Lett.* **70**, 2960 (1993).
55. Y. Fuseya, H. Kohno, and K. Miyake, *J. Phys. Soc. Jap.* **72**, 2914 (2003).